Time-varying pulmonary arterial input impedance via wavelet decomposition

ZHENG LI, BRYDON J. B. GRANT, AND BARUCH B. LIEBER
Center for Bioengineering, University of Washington, Seattle, Washington 98195; and Departments of Medicine and of Mechanical and Aerospace Engineering, State University of New York at Buffalo, Buffalo, New York 14260

Li, Zheng, Brydon J. B. Grant, and Baruch B. Lieber. Time-varying pulmonary arterial input impedance via wavelet decomposition. *J. Appl. Physiol.* 78(6): 2309–2319, 1995.— Wavelet decomposition is proposed as a novel approach for determining pulmonary arterial input impedance throughout the breathing cycle. The canine pulmonary arterial input impedance was evaluated throughout the ventilatory cycle at 5, 10, and 15 cmH_2O of positive end-expiratory pressure. The impedance spectrum was obtained by Fourier transformation of wavelets generated by decomposing the pulmonary arterial pressure and flow waveforms. With wavelet decomposition, each heart beat is viewed individually as a transient pulse rather than as an interval within a continuous function of pressure and flow. The advantage of using this approach is the ability to obtain stable estimates of input impedance spectra with high-frequency resolution over the entire frequency range with only a limited data set of pressure and flow decomposed to wavelets as short as singular extrapolated cardiac cycles. This method was used to define the changes of input impedance that occur during the ventilatory cycle. Results show that the impedance spectrum undergoes notable changes during the breathing cycle and demonstrate the utility of the proposed method.

input impedance; pulmonary circulation; wavelets

IN A PREVIOUS STUDY (7), we demonstrated that pulmonary arterial compliance (Ca) undergoes variations during the ventilatory cycle and we concluded that it is time varying. We hypothesized that pulmonary arterial input impedance also may be varying throughout the ventilatory cycle, but such variations may not have been identified because we were limited to only two specific phases of the ventilatory cycle. This matter is of importance because time variation of input impedance would impose severe restrictions on the conditions under which it is estimated.

GENERAL METHODOLOGY

The concept of input impedance explicitly assumes that the system under consideration is passive, causal, and time invariant. A system is causal if the output at any time depends only on the values of the input at the present time and in the past (11). A passive system is one that is free of energy sources besides these supplied at the input (16). In the pulmonary circulation, this assumption is not satisfied because breathing acts on the pulmonary vasculature as an external energy source. Ventilation is responsible for changes in lung volume, thus altering the geometry of blood vessels inside the lung itself (12). Changes of lung volume have differing effects on the extra-alveolar and alveolar blood vessels. These changes in lung volume result from alterations in transpulmonary pressure that are, in essence, a secondary energy source. We hypothesized that the pressure-flow relationship with respect to the cardiac cycle measured at the main pulmonary artery (i.e., input impedance) while ventilation is sustained may be time varying, because the passivity assumption is not satisfied. To examine the pressure-flow relationship with respect to the cardiac cycle, it is important to account for the slow time variations imposed on the data by ventilation or restore passivity. Thereafter, the pressure-flow relationship can be examined (or interpreted) as belonging to a piecewise linear time-invariant system.

From the viewpoint of cardiodynamics, ventilatory changes violate passivity and may be viewed as rendering the system time varying with respect to the cardiac cycle. One way to restore steady state to the system is to examine specific phases of the ventilatory cycle. For a system in steady-state oscillations, observations made in a short time window in the past are equivalent to observations made at any short time window later in time. In our case, a short time window refers to the duration of a cardiac cycle (see Fig. 1). The concept of input impedance may become tenable if the pressure-flow relationship is assumed to be time invariant with respect to the cardiac cycle only, and time-varying changes in input impedance are assumed to be occurring over phases of ventilation. During each such phase, ventilatory effects on the hemodynamics are frozen in time, and observations on consecutive heart beats at the same phase of ventilation can be considered as belonging to a passive hemodynamic system. Thus specific phases of ventilation can be considered as a collection of passive hemodynamic systems that differ from each other because of the state of distention of the lung during the ventilatory cycle. A sustained cyclical action of ventilation on the pulmonary vasculature is needed for this method. Observations on hemodynamic variables are restricted to specific phases of the ventilatory cycle, and

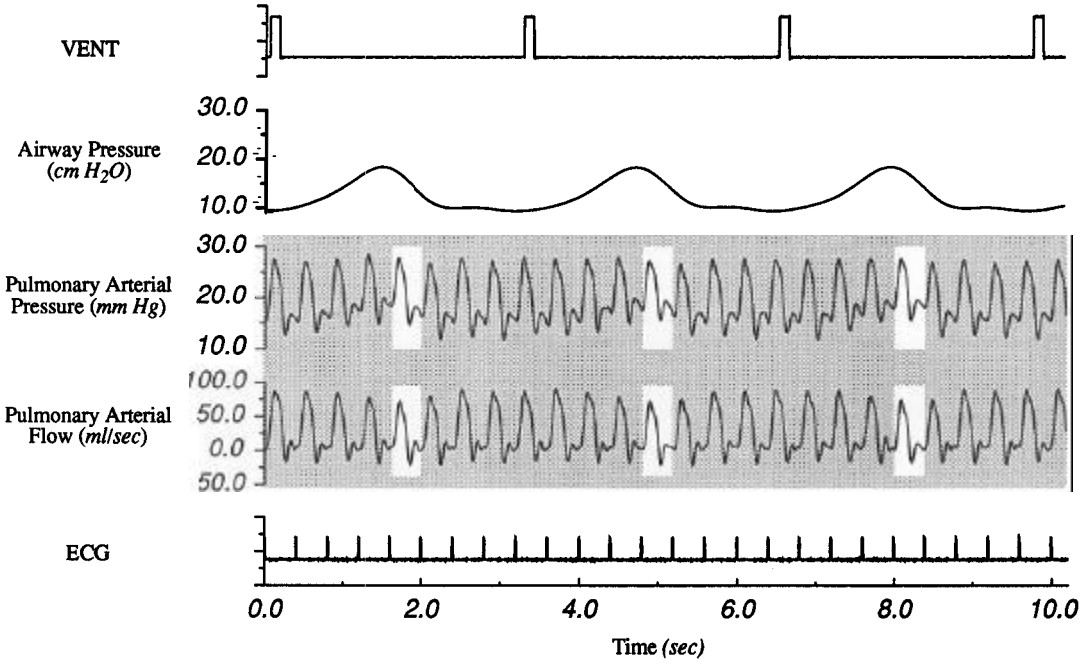

FIG. 1. Tracings of pulmonary arterial pressure, flow, airway pressure, ventilator trigger (VENT), and ECG trigger.

consecutive observations are made at the same specific phases in consecutive ventilatory cycles.

The underlying assumption is that the system is in a steady state and the ventilatory cycles are indeed repetitive. This assumption is readily satisfied when subjects are mechanically ventilated. Furthermore, it is assumed that each ventilatory cycle contains the same number of heart beats. At any particular phase of the ventilatory cycle, it is reasonable to assume that in consecutive breathing cycles lung volume and transpulmonary pressure will be virtually the same as in previous breaths. Thus, for these particular heart beats at consecutive breathing cycles, the right ventricle faces a downstream system of equivalent properties. Therefore, the system has now been rendered time invariant with respect to a specific phase of the ventilatory cycle.

Figure 1 shows the traces of pulmonary arterial pressure and flow, airway pressure, ventilator trigger, and the electrocardiogram (ECG). The unshaded windows in pulmonary arterial pressure and flow demonstrate this concept and the equivalency of the hemodynamic variables for heart beats at the onset of expiration. If heart beats at specific phases of ventilation are concatenated (10), the resulting traces can be considered as belonging to a time-invariant passive system in steady-state oscillations. This concept is demonstrated in the tracings of Fig. 2, where pressure and flow waveforms of heart beats at the onset of expiration have been collected from 15 breaths. The slow temporal variations

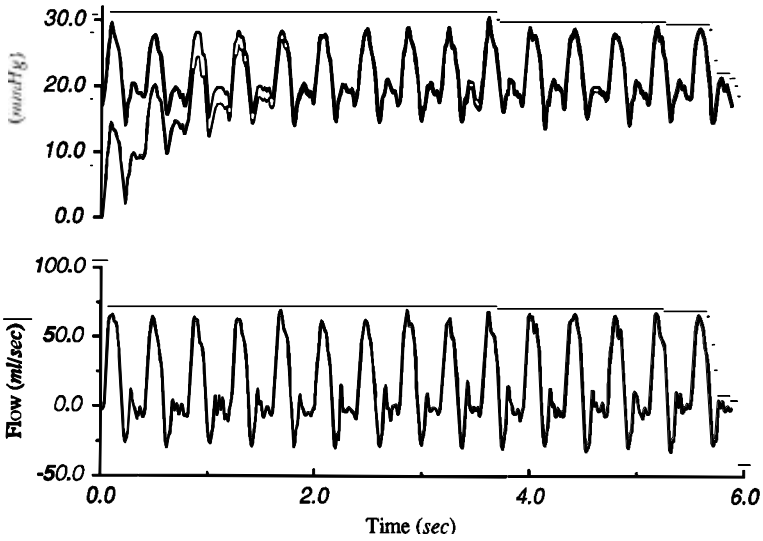

FIG. 2. Pulmonary arterial pressure and flow at beginning of expiration. Thick line (top line of pressure graph) represents experimental data and thin line represents wavelet reconstruction.

due to ventilation that are present in the tracings of Fig. 1 are absent in Fig. 2.

Naturally, this type of processing requires the collection of a number of ventilatory cycles. The number of the cardiac cycles (the fundamental frequency) in each processed data record at any specific phase of breathing will depend on the number of ventilatory cycles collected. Frequently, it is difficult to maintain the system in a steady state. Therefore, the number of cycles of the fundamental frequency is usually limited. Classic Fourier methods are hard pressed to perform well on such short data records (9). For signals composed of sinusoids in noise, short data records refer to the number of cycles of the fundamental frequency (heart rate). For example, a record is considered short if there are only 10 cycles in each of 15 segments. A different approach is required in this circumstance. A wavelet spectral method that makes use of the fast Fourier transform and is based on transients is more useful for short data records rather than classic methods for estimating the input impedance spectrum (1, 14). The wavelets, in this context, are constructed from individual heart beats that are extrapolated from measured data to represent pressure and flow in the main pulmonary artery for a hypothetical singular heart beat. The flow wavelet is essentially the regular beat zero padded beyond diastole. The extrapolation of the pressure wavelet is done by a first-order exponential decay. The extrapolation by zero padding and exponential decay also increases the frequency resolution in the subsequent transformation. Furthermore, since the fast Fourier transform is very sensitive to noise, ensemble averaging over all available wavelet pairs in the spectral domain can reduce greatly the instability of the estimates due to extraneous noise (1).

The steady-state pulsatile pressure and flow waveforms can be decomposed into wavelets for each heart beat. Pulmonary arterial flow during each cardiac cycle can be viewed readily as a transient wavelet, because blood ejection into the pulmonary vasculature occurs only during systole. Flow is essentially equal to zero at the start of systole and the end of diastole.

Pulmonary arterial pressure cannot be decomposed into the transient wavelets as simply as flow. This difference is due to the viscoelastic nature of the pulmonary vasculature that stores a portion of the pressure as potential energy in the pulmonary circulation. The pressure wavelet is generated by extrapolating the measured pressure for each heart beat effectively to zero. Therefore, the duration of a pressure wavelet must exceed the duration of the cardiac cycle. As a result, successive pressure wavelets overlap. Nevertheless, the summation of these pressure wavelets must approximate the measured pressure. A special procedure that is described below (see WAVELET DECOMPOSITION OF PRESSURE) must be used to obtain the pressure wavelets that meet these requirements, but first we must define a wavelet and obtain the input impedance by using wavelets.

INPUT IMPEDANCE BY USING WAVELETS

A wavelet (as shown in Fig. 3) of duration (T_w) is defined as a transient square integrable function that exists only within the time interval $(0,T_w)$, otherwise it is identical to zero (14).

$$f(t) = \begin{cases} f(t)\ 0 \le t \le T_w \\ 0 \quad \text{otherwise} \end{cases} \text{ and } \int_0^\infty |f(t)|^2 dt < \infty \qquad (1)$$

where t is time. Pulmonary arterial pressure [$P(t)$] can be represented as the sum of the wavelets [$P_n(t)$], which are convolved with a unit impulse function, $\delta(t)$. Similarly, pulmonary arterial flow [$\dot{Q}(t)$] can be represented as the sum of $\dot{Q}_n(t)$, which are convolved with a unit impulse function

$$\begin{aligned} P(t) &= \sum_{-\infty}^{\infty} P_n(t) * \delta(t - T_n) \\ \dot{Q}(t) &= \sum_{-\infty}^{\infty} \dot{Q}_n(t) * \delta(t - T_n) \end{aligned} \qquad (2)$$

Here T_n is the start of systole of the nth wavelet that can be identified as the minimum pressure point prior to ejection, and asterisk denotes the convolution operator. Considering the flow wavelet as an input to the system, the pressure wavelet as the response, and $h(t)$ as a linear time-invariant operator between flow and pressure wavelet, it can be shown (2) that

$$P(t) = h(t) * \dot{Q}(t) \qquad (3)$$

If we reverse the roles such that the pressure wavelet is an input to the system, flow wavelet is the response, and $a(t)$ is a linear time-invariant operator between each pressure and flow wavelet, we can similarly obtain

$$\dot{Q}(t) = a(t) * P(t) \qquad (4)$$

For linear time-invariant systems, $h(t)$ and $a(t)$ are also impulse responses of each system, and their Fourier transforms [$H(j\omega)$ and $A(j\omega)$] are the frequency responses or the transfer functions of the system. The two transfer functions are uniquely related by

$$H(j\omega) = \frac{1}{A(j\omega)} \qquad (5)$$

Here $H(j\omega)$ represents the input impedance whereas $A(j\omega)$ represents the input admittance (6). The frequency response of the system, $H(j\omega)$, can be evaluated directly or by first determining $A(j\omega)$ and then invert it to obtain $H(j\omega)$. For a truly linear time-invariant system with noiseless measured input and response, the two functions are interchangeable. In reality, however, the transfer function is unknown, and we have to evaluate it from measured input and response, which are usually contaminated with noise. In theory, the impedance or the admittance functions do not have any singularities (values of zero or infinity) in their magnitude, and evaluation of either function is permissible. Bergel and Milnor (3) demonstrated that the pulmonary bed approximates a linear system. It is also well recognized that the pulmonary input impedance approaches a finite value of the characteristic impedance and zero phase shift at high frequencies (15). Therefore, singularities are not anticipated, and evaluation of either function is possible and valid. However, the

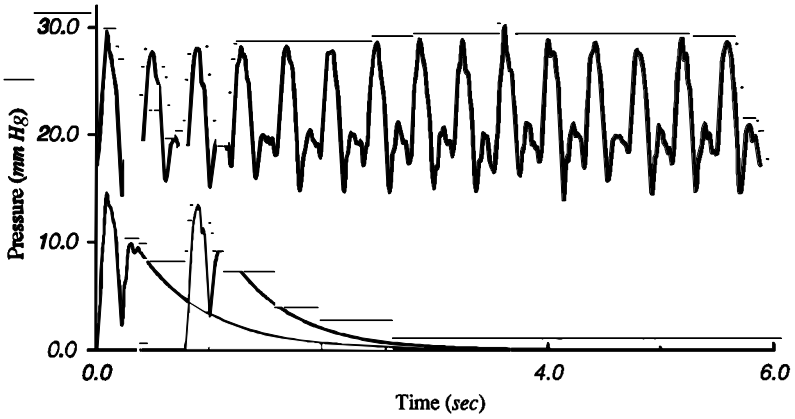

FIG. 3. Pulmonary arterial pressure at beginning of expiration and wavelet decomposition of individual beats.

presence of noise in the measured data can adversely affect the impedance estimate by making it statistically inconsistent and may introduce singularities in the estimates. In our experiments, pulmonary arterial pressure was measured with a solid-state pressure transducer, whereas pulmonary arterial flow was measured with an electromagnetic flowmeter. Consequently, flow measurements were more susceptible to noise than pressure. Under such circumstances, it is preferable to determine the input admittance first and then invert it to obtain the impedance. By evaluating the admittance first, only the autospectrum of the cleaner signal (pressure) appears in the denominator of the expression for evaluating the transfer function (see *Eq. 6*). A similar approach of using the variable with the least noise in the denominator has been suggested for estimating the slope of the linear regression by Brace (4).

For $H(j\omega)$ to be considered as the input impedance [$Z(j\omega)$], the system must be passive and in steady state. In mathematical terms, $H(j\omega)$ needs to be a positive-real function, i.e., the real part of the function needs to be positive, such that the phase angle lies within the open interval $(-\pi/2, +\pi/2)$ for all frequencies. If $Z(j\omega)$ is a positive-real function, then $Z(j\omega)$ is also a minimum-phase system (11). The minimum-phase condition uniquely relates the log of the magnitude of $Z(j\omega)$ to its phase. The log of the magnitude of $Z(j\omega)$ [log $Z(j\omega)$] and its phase arg[$Z(j\omega)$] for a minimum-phase system is called a Hilbert transform pair. Because the two are uniquely related, the phase of $Z(j\omega)$ can be reconstructed from the logarithm of the known magnitude.

Wavelet spectral methods for estimation of input impedance are based on the theory for nonstationary random data analysis contrary to classical spectral methods that assume wide-sense stationary signals (1). After the steady-state pressure and flow have been decomposed into the wavelets, the frequency response can be obtained by using nonstationary data-analysis theory. The frequency response, $H(j\omega)$ or $A(j\omega)$, of a linear time-invariant system can be estimated in the least squares sense (1) by

$$\hat{H}(j\omega) = \frac{\hat{G}_{\dot{Q}P}(j\omega)}{\hat{G}_{\dot{Q}\dot{Q}}(j\omega)}\,;\ \hat{A}(j\omega) = \frac{\hat{G}_{P\dot{Q}}(j\omega)}{\hat{G}_{PP}(j\omega)} \tag{6}$$

where hat ($\hat{}$) denotes estimated values, $G_{P\dot{Q}}(j\omega)$ is the energy cross-spectral density function between pressure and flow, $G_{\dot{Q}\dot{Q}}(j\omega)$ is the energy autospectral density function of flow, and $G_{PP}(j\omega)$ is the energy autospectral density function of pressure. An estimate of $G_{P\dot{Q}}(j\omega)$ and $G_{\dot{Q}\dot{Q}}(j\omega)$ or $G_{PP}(j\omega)$ can be obtained by the ensemble averaging the corresponding estimates for each wavelet pair (2).

When only a limited number of wavelets is available, the variance in the estimates of the magnitude and phase of $\hat{A}(j\omega)$ or $\hat{H}(j\omega)$ at higher frequencies is too large. Therefore, an alternative method was used to estimate the magnitude of $\hat{A}(j\omega)$.

$$|\hat{A}(j\omega)| = \frac{|\hat{G}_{P\dot{Q}}(j\omega)|}{|\hat{G}_{PP}(j\omega)|} \tag{7}$$

where

$$\begin{aligned} |\hat{G}_{P\dot{Q}}(j\omega)| &= \frac{1}{N}\sum_{i=1}^{N} |Q_i(j\omega)P_i^*(j\omega) \\ |\hat{G}_{PP}(j\omega)| &= \frac{1}{N}\sum_{i=1}^{N} |P_i(j\omega)|^2 \end{aligned} \tag{8}$$

Here $P_i(j\omega)$ and $Q_i(j\omega)$ are the finite Fourier transforms of the ith pressure and flow wavelets of duration T_w. $Q_i^*(j\omega)$ and $P_i^*(j\omega)$ are the complex conjugate of $Q_i(j\omega)$ and $P_i(j\omega)$, respectively, and N is the number of wavelets. An increase in the number of wavelets N will reduce the random noise factor present in beat to beat and also reduce the instability of the individual estimates of the energy spectral density functions. In our data, the instability of the magnitude of $\hat{A}(j\omega)$ was greatly reduced compared with any other classic Fourier method, even though a limited number (15) of wavelets were available. A comparison of the stability of the impedance spectra amplitudes that were obtained by Fourier transform of the wavelets and by fast Fourier transform of the continuous time record is shown in Fig. 4. The best estimate of the fast Fourier transform spectrum was obtained by ensemble averaging four subsegments of the data with 20% (one cardiac cycle) overlap in each.

As noted earlier, the phase response can be obtained theoretically from the known magnitude by using the Hilbert transform. In reality, it is difficult to estimate

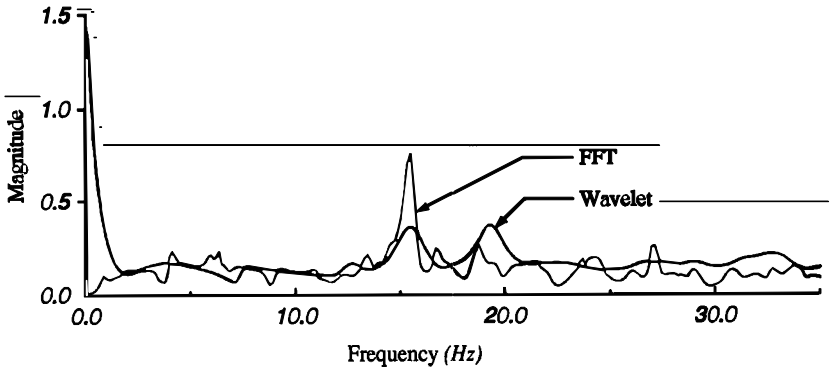

FIG. 4. Comparison of fast Fourier transform (FFT) and wavelet estimates of input impedance at onset of expiration.

the phase directly because of the singularities in this transformation. The most practical approach to estimate the phase is to use the iterative technique developed by Quatieri and Oppenheim (13) to reconstruct the phase from the magnitude. This technique is based on the minimum-phase condition noted earlier. The iterative algorithm can be described by the following: *1*) by using the estimated magnitude and by setting the initial guess for the phase angles to zero, an impulse response function can be obtained by the backward (inverse) Fourier transform; *2*) causality is imposed on the impulse response by forcing the last quarter of the transfer function values to be zero; *3*) new phase angles are calculated by forward Fourier transform of the new impulse response function; *4*) the process is repeated by returning to *step 1* while using the new phase angles from *3*, until the impulse response function and the phase angles converge.

The input impedance can be obtained by inverting the admittance. The validation of the reconstructed complete frequency response function as representing the input impedance is as follows. If the reconstructed phase angles lie within the range of $-\pi/2$ to $+\pi/2$, then the frequency response of the system, $\hat{H}(j\omega)$, is equivalent to the input impedance, $Z(j\omega)$. Otherwise, either the system is still time variant or may have other distal energy sources. Finally, the predicted steady-state pressure response $[\hat{P}(t)]$ can be calculated by taking the inverse transformation of the product of the measured flow, $\dot{Q}(j\omega)$, by the frequency response function, $\hat{H}(j\omega)$, in the frequency domain. If the predicted pressure $\hat{P}(t)$ faithfully represents the measured pressure $P(t)$, then this method successfully estimated the input impedance.

WAVELET DECOMPOSITION OF PRESSURE

When the steady-state pressure is considered as a collection of transients, the pressure signal is time aliased because of the overlap of successive transients (8). To reconstruct the pressure wavelets from the steady-state pressure, time aliasing must be removed. For the pulmonary vascular system with a relatively short input flow wavelet, we can assume that the response pressure wavelet will follow a first-order exponential decay beyond one cardiac cycle, if it was not interrupted by a new succeeding heart beat. We propose the following procedure to unalias the steady-state pressure when decomposing it into wavelets.

Let us assume an ideal case when the cardiac period (ΔT) and the value of the steady-state pressure at the onset of each systole (D) are constant. By extrapolation, the pressure wavelet after the duration of the heart beat is

$$P_i(t) = De^{-t/\tau} \text{ for } \Delta T \leq t \leq T_w \tag{9}$$

where the time constant (τ) = $\Delta T/\ln 2$. The pressure overlap within each cardiac cycle due to the long decay time of the wavelets is in fact a cumulative result of all preceding wavelets that have not completely decayed yet. The amount of overlap can be calculated by

$$P_{ol}(t) = De^{-(t+\Delta T)/\tau} + De^{-(t+2\Delta T)/\tau} + De^{-(t+3\Delta T)/\tau} + \cdots = D\frac{e^{-(t+\Delta T)/\tau}}{1 - e^{-\Delta T/\tau}} = De^{-t/\tau} \tag{10}$$

P_{ol} is the amount of overlap that needs to be subtracted from the steady-state pressure signal to obtain an approximation for the pressure wavelet within the cardiac cycle. This method guarantees a zero value for the wavelet pressure when $t = 0$ and pressure continuity when $t = \Delta T$, in addition to completion of the wavelet beyond the individual heart beat.

In practice, there is a beat-to-beat variation in both the duration of each heart beat and the value of pulmonary arterial pressure at the onset of each systole. Therefore, the time constant τ and the pressure constant for the ith wavelet (D_i) are determined by

$$D_i = P(T_i) \text{ and } \tau_i = \frac{T_{i+1} - T_i}{\ln (2P_i/P_{i+1})} \tag{11}$$

where T_i is the time at the onset of the ith heart beat.

EXPERIMENTAL METHODS

Animal preparation. The experimental preparation that we used has been described in great detail elsewhere (7). Experiments were performed on mongrel dogs in compliance with the guidelines of the American Physiological Society. The anesthetized dogs were intubated and ventilated with a volume-cycled pump (model 681, Harvard Apparatus, Natick, MA). The ventilatory rate was set at 14–18 cycles/min, with a constant tidal volume throughout each experiment. Stroke volume of the ventilator was set at ~15 ml/kg. Inspiration was achieved by positive pressure while expiration was passive. The duration time of inspiration and expiration was fixed and equal. Airway pressure was monitored with a Val-

idyne differential pressure transducer. A catheter was placed in the right femoral artery to monitor systemic arterial pressure with a Statham P23 ID pressure transducer.

The chest was open throughout the experiment, and 5 cmH_2O of positive end-expiratory pressure (PEEP) were applied to prevent atelectasis and serve as baseline. Thereafter, 10 and 15 cmH_2O were applied to simulate circulatory disturbances. The pericardium was transacted vertically, and the pulmonary artery was isolated by blunt dissection. A Statham electromagnetic flow probe (between 16 and 18 mm ID) was placed around the main pulmonary artery. Two 3-Fr micromanometer-tipped catheters (Millar, Houston, TX) were placed, through purse-string sutures, into the right ventricular outflow tract and into the pulmonary artery for simultaneous pressure measurements. All pressure calibrations were performed relative to atmospheric pressure. After instrumentation, data collection was started when the preparation was judged to be stable, as manifested by constant mean systemic pressure, pulmonary arterial pressure, and flow. Measurements were collected over a period of 15 breaths.

Data collection and analysis. All the collected analog signals were displayed on an eight-channel Gould 2800S strip-chart recorder. In parallel, all the analog signals were digitized (Data Translation DT2801A) and stored on a computer (Wells-American A Star, Columbia, SC) for off-line analysis. The sampling rate of the various pressure and flow waves was set at 250 Hz/channel. The beginning of each ventilatory cycle was recorded by using the output of a microswitch that was positioned on the ventilator and delivered a 5-V pulse at the end of expiration. The beginning of each individual heart beat was defined from a recorded pulse that was triggered by the QRS complex of the ECG (ECG/Biotech amplifier, Gould).

Data preparation. Pulmonary input impedance was estimated for each cardiac cycle throughout the ventilatory cycle. To eliminate time variations in the data to be analyzed and obtain N cardiac cycles at each phase of the ventilatory cycle, new data subsets were generated from the experimental data. By using both the ventilator trigger and the ECG trigger, consecutive cardiac cycles within each ventilatory cycle were marked, i.e., cardiac cycle $i = 1, \ldots, K$ within each ventilatory cycle $j = 1, \ldots, N$. For each i, N cardiac cycles were collected from the N successive ventilatory cycles for both pulmonary arterial pressure and flow. The result was K new subsets of pressure and flow data, each containing N cardiac cycles at particular phases of the ventilatory cycle. The method is illustrated in Fig. 1. The new data subsets were free of time variations due to ventilation, although there was a small degree of phase jitter in the newly constructed data sets because heart rate is not synchronized precisely to the ventilatory rate. Nonetheless, time variation of consecutive cardiac cycles due to ventilation in the newly constructed data sets was virtually eliminated. Because data was collected for 15 successive breaths, the new subsets contained $N = 15$ cycles of the fundamental (cardiac) frequency. These sets can be considered as obtained from a system in steady-state oscillations (without time variations) driven by a steady frequency source.

RESULTS

For clarity, the tracings were low-pass filtered in the frequency domain with a finite-duration impulse-response filter (11), the cutoff frequency of which was set to the 10th harmonic of heart rate. It has been demonstrated by Bergel and Milnor (3) that ~99% of the variance of measured pressure or flow signals in vivo is contained in the first eight harmonics of heart rate. We tested our data (17) and found that 10 harmonics of heart rate were necessary to reproduce >96% of the variance in the original signals. However, in the entire analysis, only the unfiltered tracings, which were sampled with a rate of 250 Hz, were used to avoid any loss of information contained in the data. Although such high sampling rate also introduces some artifacts, such as phase aliasing due to high frequency noise being collected with the data. Nonetheless, such artifacts are small and can be eliminated as explained subsequently in DISCUSSION.

The analysis was performed on five dogs, but for brevity results for one dog only will be illustrated in detail. Figure 2 is an example of pressure and flow waveforms collected in the start of expiration for PEEP level of 10 cmH_2O. Changes in transpulmonary pressure are most rapid at the start of expiration and, thus, should have the largest impact on the hemodynamics variables. As can be seen in Fig. 2, time variations due to ventilation have been virtually eliminated. The reconstructed pressure that was obtained by summation of the wavelets is also shown in Fig. 2 by the thin line. The reconstructed pressure becomes indistinguishable from the experimental pressure after a short transient period of five cardiac cycles. Conceptually, the transient period is the amount of time required to pump up the pressure in the system from zero to the steady-state level by successive transients. The wavelets that were used for the reconstruction in Fig. 2 are shown in Fig. 3. Only the first and the third wavelets are shown in Fig. 3, *bottom,* whereas the steady-state pressure used to generate the wavelets is depicted at the *top.* The construction of the flow wavelets is trivial, since the only modification to the steady-state flow is zero padding beyond end diastole of a heart beat. The number of data points used in each wavelet is 2,048, which allows the pressure wavelet to decay effectively to zero. A power of two was chosen for convenience when calculating fast Fourier transforms. The fact that this mathematical approach of using wavelet decomposition to calculate input impedance does predict the steady-state signal is demonstrated in Fig. 5. The predicted pressure in Fig. 5 was obtained as outlined before by inverse Fourier transformation of the product of predicted frequency response function and the experimental flow data. Figure 5 demonstrates the close agreement between measured and predicted pressure. A thorough quantitative comparison of the two pressure tracings is given in APPENDIX.

An example of the calculated amplitude and phase of the input impedance throughout the ventilatory cycle is presented for PEEP level of 5 cmH_2O (Fig. 6), 10 cmH_2O (Fig. 7), and 15 cmH_2O (Fig. 8). The results are presented in the frequency scale up to 25 Hz only. We evaluated the coherence function for each impedance data subset used in the analysis and found that coherence was generally maintained at a high value (>0.8) only up to that frequency (17). Therefore, no definitive statements can be made with regard to higher frequencies, other than that the relationship between pressure and flow at higher frequencies is highly nonlinear and may be due to high frequency noise. In all data subsets used

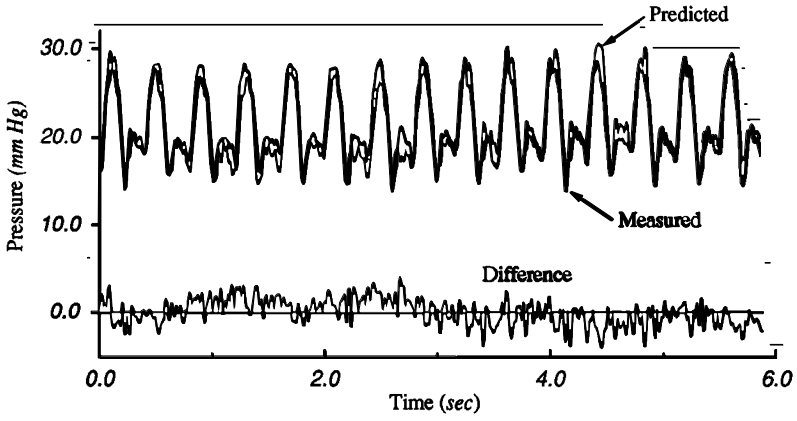

FIG. 5. Pulmonary arterial pressure at beginning of expiration and predicted pressure.

to construct the phase angles, they have been verified to lie within the open interval of $-\pi/2$ to $+\pi/2$, thus satisfying the minimum-phase assumption (17). A prominent feature of the impedance spectrum is the existence of four secondary maxima at frequencies of 6.6, 11.6, 15.1, and 19.2 Hz. These maxima are reflected in both the magnitude and the phase. The striking features of these extrema is that they are varying in magnitude during the ventilatory cycle. At the lower frequencies, the magnitude of the peaks is diminishing at the center of the ventilatory cycle when airway pressure is high.

On the other hand, the magnitude of the peaks at the higher frequencies possesses an opposite trend, and the peaks are amplified at the middle of the ventilatory cycle when airway pressure is high. This phenomenon can be explained by wave propagation and reflection. These results suggest that the apparent compliance of the intrapulmonary arteries decreases when airway pressure is high. As a result, wave speed (or its corresponding frequency) is increasing. With decrease in apparent compliance, the energy in the reflected waves is changed from low to high frequencies. Therefore, the reflected waves at higher frequencies are amplified at the expense of waves at lower frequencies.

An increase in the PEEP level results in the attenuation of the reflected waves at all frequencies, as manifested by decreasing surface variance with PEEP in each of the five dogs (Table 1). This is particularly apparent for high frequencies (Figs. 6–8). The surface characteristic impedance was not affected significantly by quasi-static changes of PEEP. However, the amplitude scale in Fig. 8 is different than that from Figs. 6 and 7 because of the fact that there is a marked increase in the input resistance. The input resistance is the zero-frequency amplitude of the impedance spectrum. Obviously, the input resistance is increasing and attains a maximum value close to the end of inspiration where airway pressure is highest. However, it is not only the reflected waves and the input resistance that are time dependent. This important point can now be

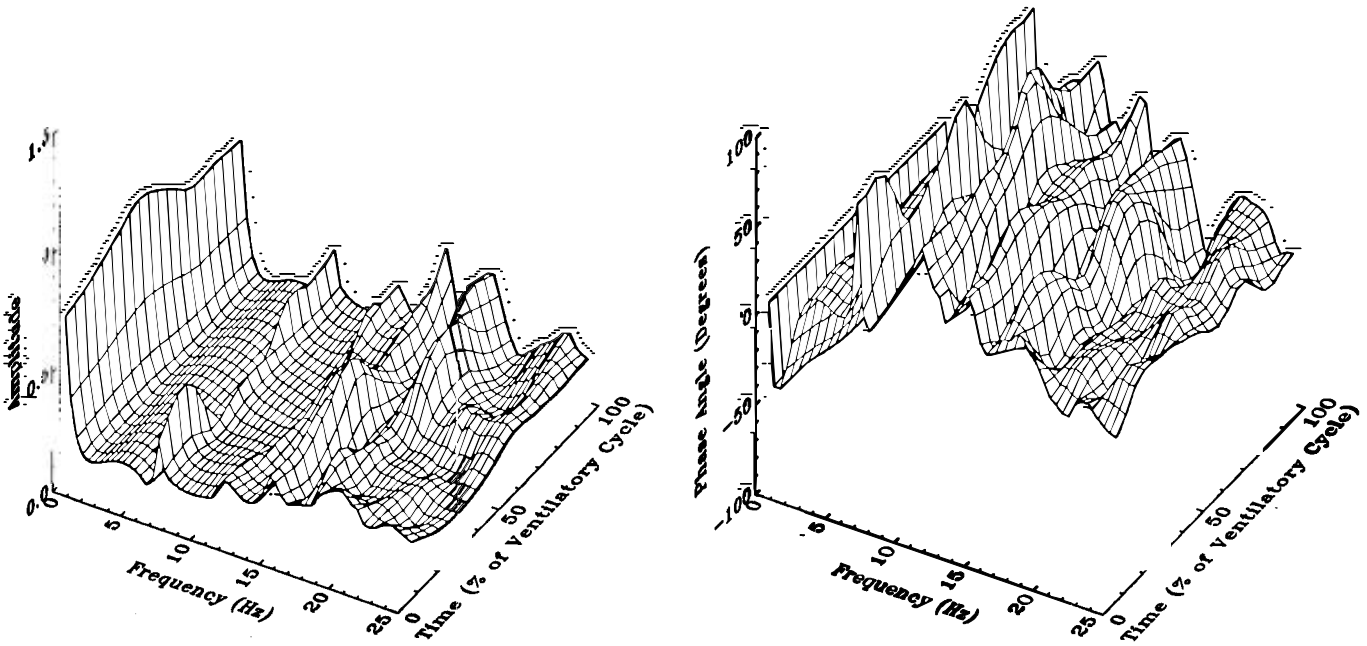

FIG. 6. Input impedance amplitude (*left*) and phase (*right*) of pulmonary circulation throughout the ventilatory cycle, PEEP = 5 cmH_2O.

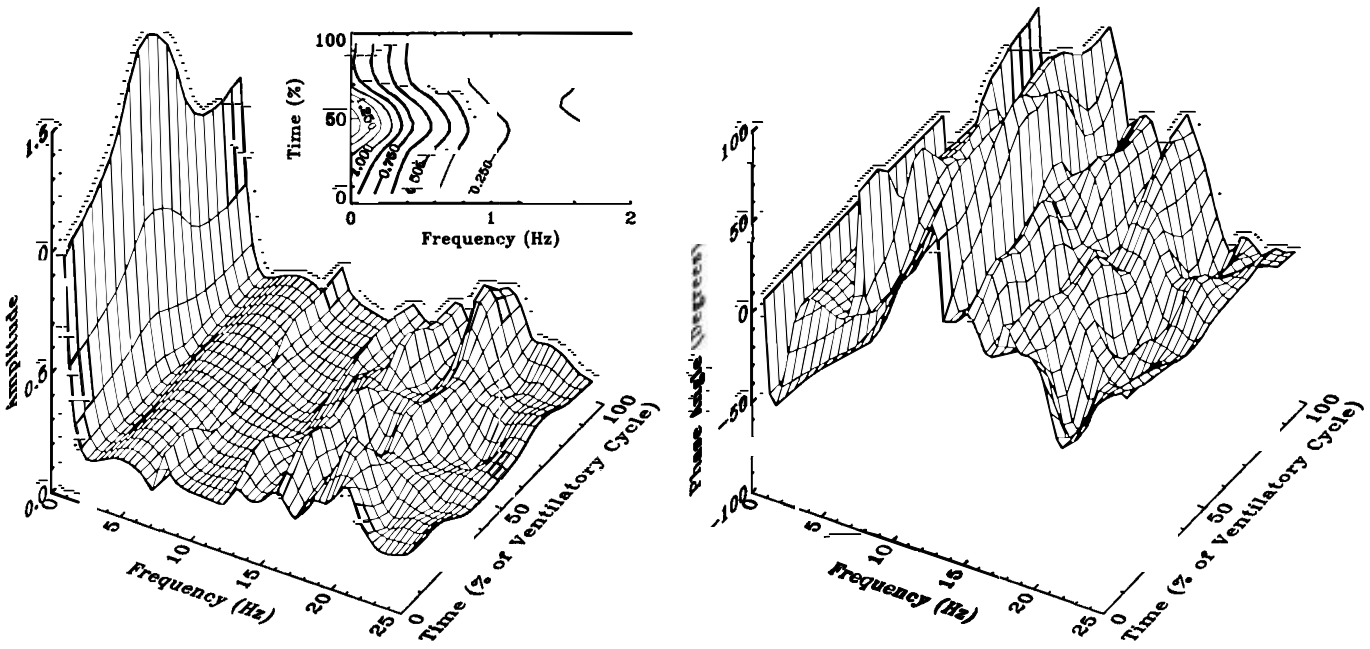

FIG. 7. Input impedance amplitude (*left*) and phase (*right*) of pulmonary circulation throughout ventilatory cycle. Contour plot *inset* at *top* of impedance amplitude at low frequencies shows that impedance and not only mean resistance are changing during ventilatory cycle; positive end-expiratory pressure (PEEP) = 10 cmH_2O.

clearly demonstrated by the contour plot insert in Fig. 7, where the variation in the magnitude of the input impedance for the first 2 Hz is shown. Therefore, not only the input resistance but also input impedance changes considerably during the ventilatory cycle.

DISCUSSION

The wavelet method provides a novel approach for estimating the input impedance when relatively short data records are available. It is particularly useful when attempting to elucidate pulmonary arterial input impedance that is varying during the ventilatory cycle. In practice, it is difficult to obtain long steady-state data records even in well-controlled animal experiment, let alone in humans. Even if as many as 15 ventilatory cycles are recorded, 15 cardiac cycles are obtained in one particular phase of ventilation. Such a record is too short for classic methods to obtain good spectral resolution with a reasonable variance. Only

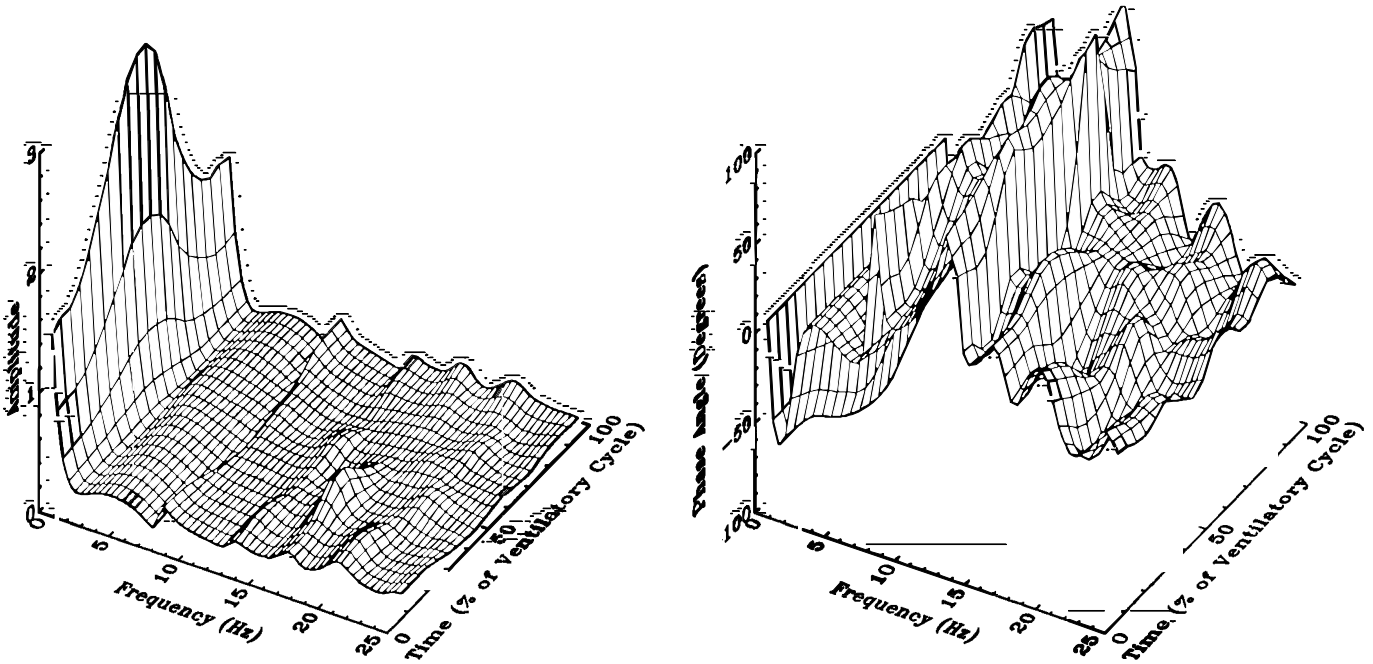

FIG. 8. Input impedance amplitude (*left*) and phase (*right*) of pulmonary circulation throughout ventilatory cycle, PEEP = 15 cmH_2O.

TABLE 1. *Surface characteristic impedance and variance at different PEEP levels in five dogs*

Dog No.	PEEP, cmH_2O	Surface Characteristic Impedance, $mmHg \cdot ml^{-1} \cdot s$	Normalized Surface Mean at High Frequencies, $2 < f(Hz) < 25$	Normalized Surface Variance at High Frequencies $2 < f(Hz) < 25$
	5	0.191440	0.154811	0.011800
1	10	0.166670	0.120806	0.005537
	15	0.126277	0.072576	0.002826
	5	0.215893	0.286681	0.021197
2	10	0.205618	0.237199	0.012055
	15	0.217227	0.186817	0.008639
	5	0.142041	0.306310	0.010005
3	10	0.085396	0.161902	0.002911
	15	0.080599	0.119657	0.002170
	5	0.178139	0.203940	0.004239
4	10	0.165288	0.159375	0.003311
	15	0.185647	0.092806	0.001094
	5	0.210155	0.285791	0.013032
5	10	0.188861	0.172336	0.004486
	15	0.167245	0.087367	0.000775

Surface characteristic impedance is average of input impedance magnitude with respect to both time of ventilatory cycle and frequency in the range $2 < f(Hz) < 25$. Normalized values are with respect to average input resistance during ventilatory cycle. PEEP, positive end-expiratory pressure.

harmonic analysis can be obtained. The advantage of the wavelet method is that a reasonable spectral estimate of high-frequency resolution can be obtained for each cardiac cycle. Ensemble averaging over the available cycles then provides the means to reduce the variance of the estimate and obtain a stable spectrum. However, a difficulty arises because of the fact that the pulmonary arterial pressure is time aliased.

Wavelet decomposition method allows one to examine the pulmonary arterial pressure-flow relationship at specific phases of the ventilatory cycle. In the method proposed by Bennett (2), input impedance is calculated by averaging over the wavelets from all phases of the ventilatory cycle. Although this method is valuable in identifying interaction caused by respiration, our approach can go one step further; namely, it provides a vehicle to reveal details of how respiration affects input impedance. Furthermore, the input impedance estimated by this method is consistent with the impedance concept that the system under study must be linear and time invariant.

Time aliasing of the pressure signal required the introduction of an assumption that extrapolates the pressure wavelet with a first-order exponential decay beyond end diastole. Mathematically, it is valid to decompose the steady-state pressure into wavelets by using our proposed method under conditions of strictly stationary data and constant heart rate. However, in reality, heart rate variability and nonrepeatability of pulmonary arterial pressure at the onset of each systole may introduce some artifacts in the estimated input impedance, particularly at high frequencies. Nonetheless, it is a small penalty to obtain a reliable high-resolution impedance spectrum, since physiologically it is the low (<10 harmonics of heart rate) frequency range that is of interest.

Wavelet decomposition has the advantage that it avoids the necessity of performing the various mathematical contortions required by the standard approach of detrending and tapering to avoid leakage that distorts the data considerably (5, 7). At first sight, the question of a pressure wavelet is of concern because it is untenable physiologically. If pulmonary arterial pressure is allowed to decay, it will not fall to zero. The wavelet is not intended to simulate a real event but provides merely a method of representing a waveform. The justification for using pressure wavelets is that their summation actually reflects the recorded pressure waves. The extrapolated data is not extraneous, it is merely an alternative way of generating zero diastolic pressure. For Fourier analysis, the mean is subtracted from each data point. This concept is readily acceptable because of our familiarity with it. Both approaches are valid, the wavelet is less easy to calculate than the mean, but it has the advantage that it is subject to less restrictions.

High-frequency resolution input impedance is particularly important in attempting to calculate the distance of reflection sites, because the precise frequencies of local extrema must be known first. The extrapolation of the pressure waveform required to produce the wavelets might be considered to introduce spurious data into the analysis and distort the impedance spectrum. However, it should be emphasized that with our method of analysis the summation of the wavelets reproduces the measured pressure recording precisely.

The method of analysis for phase reconstruction makes use of timespectral transformations repeatedly. Therefore, to obtain accurate estimates of the transfer function and the phase of the frequency-response function, the iterative algorithm must make use of the magnitude over the entire frequency range (up to 125 Hz in our data for a sampling rate of 250 Hz). The high sampling rate is particularly important in minimizing the truncation error when an inverse Fourier transform is applied to obtain the impulse response function. However, the magnitude of the frequency response function at high frequencies (>10 harmonics of the heart rate) is usually biased because of noise in the original signals. Depending on the noise level, a small time shift occurs between the predicted and the measured pressure due to the flowmeter and slight differ-

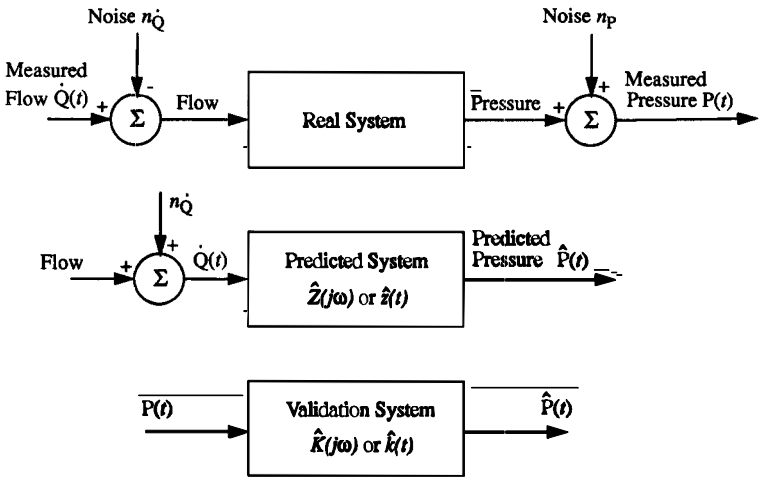

FIG. 9. Block diagram of a procedure to compare predicted system response with measured data. See text for symbol definitions.

ences in the alignment between the pressure and flow transducers. The precise time shift can be easily determined by evaluating the cross-correlation function between the experimental and predicted pressure. Usually, this time shift amounted only to 0.004–0.016 s. Nonetheless, it is necessary to correct the phase response of the input impedance in the frequency domain in such situations to avoid phase aliasing.

In summary, the wavelet method is a powerful tool in evaluation of pulmonary input impedance, since it relies on nonstationary processes theory and thus is more suitable for analyzing pulmonary hemodynamics that are rendered nonstationary by ventilation. Furthermore, it is capable of estimating input impedance with a high-frequency resolution that will be helpful for studying wave reflection. To calculate the distance of the reflection sites from the origin of the pulmonary artery, it is important to locate the frequencies with maximum or minimum precisely.

APPENDIX

In general, the measured steady-state pressure $P(t)$ and the predicted steady-state pressure $\hat{P}(t)$ will be very similar. Nonetheless, all the quantities involved in the estimation of the frequency-response function of the pulmonary vasculature contain an unknown and inseparable amount of error in them (see Fig. 9, *top*). The measured flow $\dot{Q}(t)$ and the measured pressure $P(t)$ contain noise components $n_{\dot{Q}}$ and n_P, respectively. $n_{\dot{Q}}$ and n_P may (or may not) be partially correlated depending on the experimental preparation and conditions, data-acquisition system, or laboratory electronic circuitry. Therefore, the predicted frequency-response function, $\hat{Z}(j\omega)$, is only an estimate of the actual function.

When the estimated transfer function of the system is convolved with the measured flow to produce the predicted pressure, the noise in the measured flow undergoes the $\hat{Z}(j\omega)$ transformation. It contaminates the predicted pressure in an unknown way. Therefore, to evaluate the quality of the $\hat{Z}(j\omega)$ by comparing the measured and predicted pressures, caution should be exercised, since both contain random errors.

The two pressure sequences (measured and predicted) are considered, respectively, the input and output of another system, which is called the validation system. We assume that these two sequences were generated as outputs by the same system and they differ from each other only because of extraneous noise. The measured sequence is contaminated by n_P, whereas the predicted sequence is contaminated by a transformation of $n_{\dot{Q}}$ through the predicted system. The most reasonable hypothesis in such a case is that the frequency-response function of the validation system, $K(j\omega)$, should be of unit magnitude and a zero phase for all frequencies within a bandwidth of interest.

In reality, however, these two sequences represent outputs from two systems that are only nearly identical. This is due to the fact that $\hat{Z}(j\omega)$ is only an estimate of the actual unknown input impedance. Therefore, a small deviation from unit magnitude and zero phase of $K(j\omega)$ is expected. If $K(j\omega)$ deviates less than an arbitrary preset value from unit magnitude and zero phase over a bandwidth of interest, the estimate of $\hat{Z}(j\omega)$ should be accepted. Otherwise we may reject it.

The problem that arises from this approach is the need to evaluate a frequency-response function for two short data records for the purpose of error analysis alone. One way to determine the transfer function of the validation system is to apply again wavelet decomposition to the two pressure sequences. However, to avoid the erroneous perception of a circular problem, it would be preferable to obtain this transfer function by another independent method. Autoregressive modeling can be used to obtain an estimate of the frequency-response function between the two pressure sequences and the coherence function (7).

In its simplest form, the criterion of assessing how close is the magnitude of $K(j\omega)$ to unity and its phase close to zero is by averaging $K(j\omega)$ and $\arg[K(j\omega)]$ over the bandwidth B of interest. In physiological applications in vivo, the bandwidth of interest is usually <10 cardiac harmonics

$$\bar{M} = \frac{1}{B}\int |K(j\omega)|\,d\omega \qquad (A1)$$

$$\overline{Ph} = \frac{1}{B}\int_B \arg[K(j\omega)]d\omega \qquad (A2)$$

where $\bar{M}$ and $\overline{Ph}$ are mean magnitude and phase, respectively, $\arg[K(j\omega)]$ is expressed in radians, and the errors in the estimates of the means (ϵ) are given by

$$\epsilon_M = \left[\frac{1}{B}\int_B (|K(j\omega)| - \bar{M})^2 d\omega\right]^{1/2} \qquad (A3)$$

$$\epsilon_{Ph} = \left[\frac{1}{B}\int_B (\arg[K(j\omega)] - \overline{Ph})^2 d\omega\right]^{1/2} \qquad (A4)$$

As an example, for the tracings shown in Fig. 5, $\overline{M} = 0.98$, $\epsilon_M = 0.08$, $\overline{Ph} = 0.24$, and $\epsilon_{Ph} = 0.09$.

It is important to note, however, that any calculated frequency-response function is only an estimate of the actual function that in most cases is unknown. Any estimated frequency-response function contains errors in the estimated values, regardless of the method by which it was obtained. These errors are due to either the modeling process by which it was obtained (e.g., autoregressive modeling) or due to the inherent large variance in the estimates when obtained by Fourier methods. The errors in the estimated values can be quantified but they are functions of frequency rather than simply scalars.

The normalized random error involved in the estimation of the magnitude of the frequency response function can be obtained as follows (1)

$$\epsilon = \frac{[1 - \gamma^2(f)]^{1/2}}{|\gamma(f)|\sqrt{2n}} \qquad (A5)$$

where $\gamma^2(f)$ is the coherence function and n is the number of segments used in the ensemble for obtaining the smoothed estimate of the frequency-response function. The SD of the estimated phase angles of the transfer function at any frequency is approximated by the same *Eq. A5*.

This work was supported in part by the National Heart, Lung, and Blood Institute Grant RO1 HL-41011.

Address for reprint requests: Z. Li, Center for Bioengineering, Univ. of Washington, Seattle, WA 98195.

Received 12 July 1993; accepted in final form 31 January 1995.

REFERENCES

1. **Bendat, J. S., and A. G. Piersol.** *Random Data: Analysis and Measurement Procedures.* New York: Wiley, 1986, p. 11, 182, 294, and 471.
2. **Bennett, S. H.** Modeling methodology for vascular input impedance determination and interpretation. *J. Appl. Physiol.* 76: 455–484, 1994.
3. **Bergel, D. H., and W. R. Milnor.** Pulmonary vascular impedance in the dog. *Circ. Res.* 16: 401–415, 1965.
4. **Brace, R. A.** Fitting straight lines to experimental data. *Am. J. Physiol.* 233 (*Regulatory Integrative Comp. Physiol.* 2): R94–R99, 1977.
5. **Brigham, E. O.** Applying the discrete Fourier transform. In: *The Fast Fourier Transform.* Englewood Cliffs, NJ: Prentice-Hall, 1974, p. 132–146.
6. **Fung, Y. C.** *Biodynamics: Circulation.* New York: Springer-Verlag, 1984, p. 363.
7. **Grant, B. J. B., J. M. Fitzpatrick, and B. B. Lieber.** Time-varying pulmonary arterial compliance. *J. Appl. Physiol.* 70: 575–583, 1991.
8. **Latson, R., W. C. Hunter, D. Burkoff, and K. Sagawa.** Time sequential prediction of ventricular-vascular interaction. *Am. J. Physiol.* 251 (*Heart Circ. Physiol.* 20): H1341–H1353, 1986.
9. **Lieber, B. B., and D. P. Giddens.** Autoregressive spectral estimation in transitional pulsatile flow. *Exp. Fluids* 8: 209–215, 1989.
10. **Lieber, B. B., Z. Li, and B. J. B. Grant.** Beat-by-beat changes of viscoelastic and inertial properties of the pulmonary arteries. *J. Appl. Physiol.* 76: 2348–2355, 1994.
11. **Oppenheim, A. V., and R. W. Schafer.** *Digital Signal Processing.* Englewood Cliffs, NJ: Prentice-Hall, 1975, p. 17, 252, 345.
12. **Permutt, S., B. Bromberger-Barnea, and N. H. Bane.** Alveolar pressure, pulmonary venous pressure, and the vascular waterfall. *Med. Thorac.* 19: 239–260, 1962.
13. **Quatieri, T. F., and A. V. Oppenheim.** Iterative techniques for minimum phase signal reconstruction from phase or magnitude. *IEEE Trans. Acoustics Speech Signal Proc. ASSP* 29: 1187–1193, 1981.
14. **Robinson, E. A.** *Random Wavelets and Cybernetic Systems.* New York: Hafner, 1962.
15. **Westerhof, N., P. Sipkema, G. Elzinga, J. P. Murgo, and J. P. Giolma.** Arterial impedance. In: *Quantitative Cardiovascular Studies,* edited by N. H. C. Hwang, D. R. Gross, and D. J. Patel. Baltimore, MD: University Park, 1979, p. 111–150.
16. **Zemanian, A.** Distribution theory and transform analysis. New York: Dover, 1987.
17. **Li, Z.** *Ventilatory Effects on Pulmonary Arterial Input Impedance: Use of Lumped-Parameter Models and Wavelet Decomposition* (PhD thesis). Buffalo, NY: State Univ. of New York at Buffalo, 1994.